

LETTER • OPEN ACCESS

Role of sea surface temperature patterns for the Southern Hemisphere jet stream response to CO₂ forcing

To cite this article: Tom Wood *et al* 2021 *Environ. Res. Lett.* **16** 014020

View the [article online](#) for updates and enhancements.

You may also like

- [Global mean thermosteric sea level projections by 2100 in CMIP6 climate models](#)
Svetlana Jevrejeva, Hindumathi Palanisamy and Luke P Jackson
- [Controls of the transient climate response to emissions by physical feedbacks, heat uptake and carbon cycling](#)
Richard G Williams, Paulo Ceppi and Anna Katavouta
- [CMIP6 projects less frequent seasonal soil moisture droughts over China in response to different warming levels](#)
Sisi Chen and Xing Yuan

ENVIRONMENTAL RESEARCH
LETTERS

LETTER

OPEN ACCESS

RECEIVED

24 August 2020

REVISED

11 November 2020

ACCEPTED FOR PUBLICATION

26 November 2020

PUBLISHED

23 December 2020

Original content from
this work may be used
under the terms of the
[Creative Commons
Attribution 4.0 licence](#).

Any further distribution
of this work must
maintain attribution to
the author(s) and the title
of the work, journal
citation and DOI.

Role of sea surface temperature patterns for the Southern Hemisphere jet stream response to CO₂ forcing

Tom Wood , Christine M McKenna , Andreas Chrysanthou and Amanda C Maycock

School of Earth and Environment, University of Leeds, Leeds, United Kingdom

E-mail: pm11tw@leeds.ac.uk**Keywords:** climate change, atmospheric circulation, jet streams, climate models, sea surface temperaturesSupplementary material for this article is available [online](#)

Abstract

The Southern Hemisphere (SH) eddy-driven jet stream has been shown to move poleward in climate models in response to greenhouse gas forcing, but the magnitude of the shift is uncertain. Here we address the fact that the latest Coupled Model Intercomparison Project phase 6 (CMIP6) models simulate, on average, a smaller jet shift in response to an abrupt quadrupling in CO₂ than the predecessor models (Coupled Model Intercomparison Project phase 5 (CMIP5)), despite producing larger global average surface warming. We focus on the response in the first decade when the majority of the long-term jet shift occurs and when the difference between CMIP5 and CMIP6 models emerges. We hypothesise the smaller poleward jet shift is related to the weaker increase in the meridional sea surface temperature (SST) gradient across the southern extratropics in CMIP6 models. We impose the multi-model mean SST patterns alongside a quadrupling in CO₂ in an intermediate complexity general circulation model (IGCM4) and show that many of the regional and seasonal differences in lower tropospheric zonal winds between CMIP5 and CMIP6 models are reproduced by prescribing the SST patterns. The main exception is in austral summer when the imposed SST patterns and CO₂ increase in IGCM4 produce weaker differences in zonal wind response compared to those simulated by CMIP5/6 models. Further IGCM4 experiments that prescribe only SH extratropical SSTs simulate a weaker jet shift for CMIP6 SSTs than for CMIP5, comparable to the full experiment. The results demonstrate that SH SST patterns are an important source of uncertainty for the shift of the midlatitude circulation in response to CO₂ forcing. The study also provides an alternative explanation than was proposed by Curtis *et al* (2020 *Environ. Res. Lett.* 15 64011), who suggested model improvements in jet biases could account for the smaller jet shift in CMIP6 models in the extended austral winter season.

1. Introduction

The Southern Hemisphere (SH) eddy-driven jet (EDJ) has been shown in climate models to strengthen and shift poleward in response to greenhouse gas (GHG) forcing (e.g. Lu *et al* 2007, Barnes *et al*, 2013). Changes in EDJ latitude and intensity—and associated changes in the Southern Annular Mode—impact on SH regional climates, including temperature and rainfall patterns over South America, southern Africa, Australia, and New Zealand (e.g. Gillett *et al* 2006, Karpechko *et al* 2009, Kang *et al* 2011, Lim *et al* 2016), as well as causing impacts on the Southern Ocean (e.g. Ferreira *et al* 2015) and Antarctic sea ice (Holland *et al*

2017). Although the sign of the SH jet shift to GHG forcing is robust across most climate models, the magnitude is uncertain with a large spread across models (e.g. Grise and Polvani 2014, 2016). The jet shift also varies regionally and seasonally (Vaughan *et al* 2020).

The spread in magnitude of the SH jet shift due to GHG forcing has been linked to the simulated pattern and magnitude of tropospheric warming and stratospheric cooling via changes in large-scale meridional temperature gradients (e.g. Harvey *et al* 2014, Grise and Polvani 2017, Bracegirdle *et al* 2018, Wood *et al* 2020a). In the CMIP5 (Coupled Model Intercomparison Project phase 5; Taylor *et al* 2012) models, intermodel spread in the effective climate sensitivity

(ECS), which is highly correlated with global surface air temperature (GSAT) change in response to an abrupt quadrupled- CO_2 ($4\times\text{CO}_2$) perturbation, could explain $\sim 25\%$ of the spread in annual mean SH jet shift on centennial timescales (Grise and Polvani 2014, 2016). More recent work shows that almost all of the long-term poleward shift in the SH jet in an abrupt $4\times\text{CO}_2$ experiment occurs in the first decade (Grise and Polvani 2017, Ceppi *et al* 2018), despite only around two thirds of the GSAT increase being realised over this period. This behaviour can be explained by the evolving pattern of sea surface temperatures (SSTs), and in particular the initial slower warming of the Southern Ocean compared to the tropical oceans (Ceppi *et al* 2018).

It has been reported that many CMIP6 (Coupled Model Intercomparison Project phase 6; Eyring *et al* 2016) models show a larger ECS than the previous CMIP5 generation (Forster *et al* 2020); indeed, multiple CMIP6 models have an ECS of ~ 5.5 K, while in CMIP5 the highest value was ~ 4.7 K (Andrews *et al* 2012). This raises the important question of how a higher ECS affects projections of regional climate change. Given the relationship between ECS and SH jet shift in CMIP5 models (Grise and Polvani 2014), it is possible that the CMIP6 models might show, on average, a larger poleward jet shift. However, Curtis *et al* (2020) showed that in the zonal mean, the average SH jet shift under abrupt $4\times\text{CO}_2$ forcing is smaller in CMIP6 models than in CMIP5. They propose that this is related to improvements in model climatology, with the systematic equatorward bias in the SH jet being smaller in CMIP6. Biases in the SH jet latitude have been shown to be statistically related to the magnitude of the jet shift in austral winter (Simpson and Polvani 2016), so the differences between CMIP5 and CMIP6 models identified by Curtis *et al* (2020) appear to be consistent with the emergent constraint relationship in that season. Curtis *et al* (2020) also found smaller but significant differences in SH jet shift between CMIP5 and CMIP6 models in austral summer, but intermodel differences in jet shift in this season are not linearly correlated with jet latitude bias (Simpson and Polvani 2016), suggesting the emergent constraint cannot explain this difference.

In this study, we examine an alternative hypothesis for the reduced poleward shift of the SH jet in CMIP6 models. Motivated by the known importance of the evolving SST response for the jet shift (Ceppi *et al* 2018), we investigate the role of differences in SST patterns simulated by the two generations of models. We further extend the work of Curtis *et al* (2020) by examining the regional differences in SH jet response in the Pacific, Atlantic and Indian Ocean basins, as earlier studies have shown these can show different behaviours (e.g. Bracegirdle *et al* 2013, Waugh *et al* 2020).

2. Methods and data

Data from 28 CMIP5 and 24 CMIP6 coupled atmosphere-ocean models (table S1, which is available online at stacks.iop.org/ERL/16/014020/mmedia) were downloaded from the Earth System Grid Federation and the UK Centre for Environmental Data Analytics JASMIN cluster. All fields were regridded using bilinear interpolation onto a common $2.5^\circ \times 2.5^\circ$ longitude-latitude grid. For both CMIP5 and CMIP6 we analyse the abrupt- $4\times\text{CO}_2$ experiment, which is initialised from the model's preindustrial control (piControl) simulation and integrated for at least 140 years. The abrupt- $4\times\text{CO}_2$ experiment is compared to the mean of the first 200 years of the piControl simulation. The CMIP5 models analysed here are very similar ($>90\%$ overlap) to the ensembles used by Grise and Polvani (2017) and Ceppi *et al* (2018). The models we analyse are also strongly overlapping with Curtis *et al* (2020). We use one additional CMIP5 model and Curtis *et al* (2020) use 11 additional CMIP6 models that we were unable to include due to missing surface temperature ('ts') fields required as input to the general circulation model experiments described later. Nevertheless, our results regarding the difference in SH EDJ shift between CMIP5 and CMIP6 are consistent with the findings of Curtis *et al* (2020). To calculate the rapid adjustment in the SH EDJ due to CO_2 —i.e. the response in the absence of changes in SSTs (Wood *et al* 2020a)—we also analyse the fixed-SST experiments with quadrupled- CO_2 (sstClim- $4\times\text{CO}_2$ and piClim- $4\times\text{CO}_2$ in CMIP5 and CMIP6, respectively, see table S1).

The latitude of the EDJ, ϕ_{EDJ} , is calculated by cubically interpolating the zonal mean zonal wind at 850 hPa onto a 0.01° latitude grid, then finding the location of the maximum wind speed between 15°S and 70°S . Diagnosing ϕ_{EDJ} using the location of the centroid of the 850 hPa zonal wind distribution (e.g. Ceppi *et al* 2018) yields qualitatively similar results, but we use the cubic interpolation method as it enables a direct comparison with recent related studies (e.g. Curtis *et al* 2020). The jet speed is diagnosed as the 850 hPa zonal mean zonal wind speed at ϕ_{EDJ} .

Meridional tropics-to-pole tropospheric temperature gradient changes are calculated by the difference between the area-average SH polar (60°S – 90°S) and tropical (30°S – 30°N) regional temperature anomalies at specific pressure levels (e.g. 850 hPa, 500 hPa and 250 hPa). To help remove the effect of differences in ECS and thus enable comparison, each model's temperature gradient anomalies are normalised by their respective GSAT change.

Following Ceppi *et al* (2018), we decompose the 'TOTAL' climate response in the abrupt- $4\times\text{CO}_2$ experiment, defined as the average over years 121–140, into a 'FAST' response averaged over years 5–10

and a ‘SLOW’ response that is the TOTAL response minus the FAST response. We focus on understanding the role of SST patterns in the FAST period as almost all of the eventual centennial jet shift occurs then. While the FAST response represents the climate anomalies averaged over only a 6 year period, we focus on the multi-model mean (MMM) differences over a large number of models, so the influence of internal climate variability will be smoothed out leaving the average forced response.

To isolate the role of SST patterns for the SH circulation response in the abrupt-4×CO₂ experiment, we perform simulations with the Intermediate Global Circulation Model version 4 (IGCM4; Joshi *et al* 2015). IGCM4 originated as the baroclinic model of Hoskins and Simmons (1975), which—along with subsequent model versions—has been used in many studies of atmospheric dynamics (e.g. Thorncroft *et al* 1993, Winter and Bourqui 2011, O’Callaghan *et al* 2014). The model simulates the major physical processes included in state-of-the-art climate models (e.g. clouds, convection, evaporation, radiation, gravity wave drag) albeit in a more simplified manner. While the SH EDJ is equatorward biased in IGCM4, this is common even in state-of-the-art climate models (e.g. Bracegirdle *et al* 2013). The model is atmosphere-only, with a horizontal spectral resolution of T42 (~2.8°) and 35 vertical sigma levels extending from the surface up to approximately 0.1 hPa (~65 km). SSTs are prescribed over the ocean surface, and while there is no explicit sea ice field its effects on key surface properties (e.g. albedo) are parameterised through the SST field by assuming a linear change in these properties between 0 °C and −2 °C. Surface temperatures over land are calculated interactively from the surface heat fluxes at each time-step.

Five 120 year long simulations were performed following a 5 year spin-up period (Wood *et al* 2020b). The simulations have fixed boundary conditions and the results show average anomalies over 119 complete seasons. In the control simulation (CTRL) we prescribe an annually repeating cycle of climatological monthly mean SSTs using the MMM of the ‘ts’ field for the first 200 years of the CMIP5 piControl simulations. Following the CMIP6 protocol (Eyring *et al* 2016), GHG (CO₂, CH₄, and N₂O) concentrations are set at preindustrial (year 1850) values and ozone is prescribed as a zonally averaged monthly mean preindustrial climatology. In two perturbation simulations (4×CO₂-FULL_{CMIP5} and 4×CO₂-FULL_{CMIP6}) the same boundary conditions are used as in CTRL, but with an annually repeating cycle of climatological monthly mean SST anomalies added using the MMM ‘ts’ field for either the CMIP5 or CMIP6 FAST responses. These SST anomalies are presented later in section 3 (figure 4). In both the 4×CO₂-FULL_{CMIP5} and 4×CO₂-FULL_{CMIP6} simulations CO₂ is quadrupled from its preindustrial

concentration. This enables a like-for-like comparison with the CMIP5 and CMIP6 abrupt-4×CO₂ simulations. Two further perturbation simulations (SHET-only_{CMIP5} and SHET-only_{CMIP6}) are used to isolate the effect of differences in SH extratropical SST patterns alone. In both simulations CO₂ is kept at preindustrial values, and CTRL SSTs are used with the SST anomalies from either 4×CO₂-FULL_{CMIP5} or 4×CO₂-FULL_{CMIP6} added poleward of 18°S. Similarly to McCrystall *et al* (2020), the SST anomalies are smoothed between 18°S and 29°S using a cosine squared weighting function with weights of 0 at 18°S and 1 at 29°S. This minimizes sharp gradients in SST across the tropical-extratropical boundary.

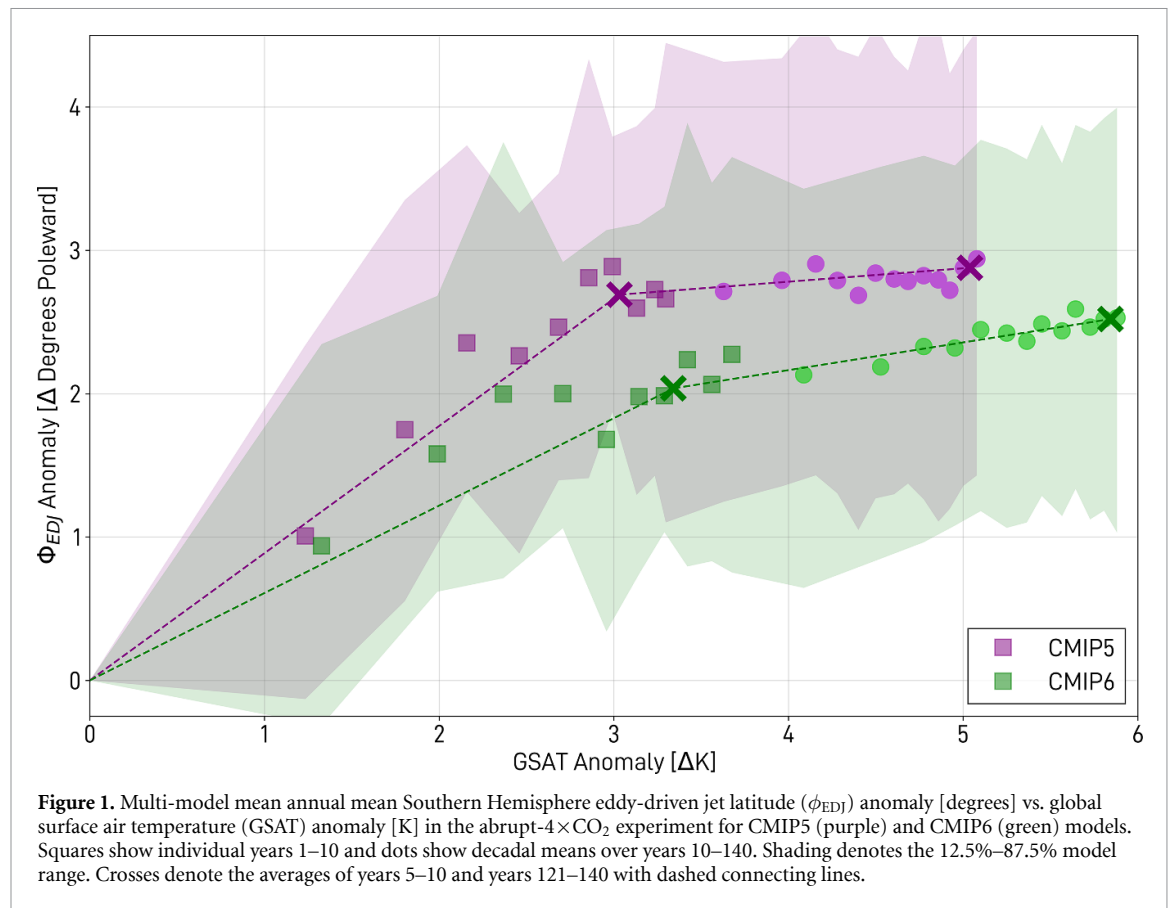
To isolate the effect of changing SST patterns alone, in all perturbation simulations we keep sea ice fixed at preindustrial values by only adding SST anomalies where the MMM sea ice concentration in the CMIP5 piControl simulations is less than 15% (i.e. equatorward of the sea ice edge). Furthermore, to remove the effect of differences in the change in global mean SST—a proxy for differences in mean ECS in the different model ensembles—the SST anomalies in each CMIP model are normalised by the respective global mean SST anomaly and then scaled to a global mean value of 2.2 K (the pooled MMM of CMIP5 and CMIP6). The MMM FAST SST anomalies from CMIP5 and CMIP6 are added to the CMIP5 preindustrial control SSTs, so as to isolate the effect of differences in the fast SST responses between CMIP5 and CMIP6, and not the effect of differences in the base state.

The statistical significance of the differences between the CMIP5 and CMIP6 models is tested using a Welch’s t-test (significant where $p < 0.05$) with the null hypothesis that the distributions of values for the two multi-model ensembles are statistically indistinguishable. The statistical significance of the IGCM4 responses is tested using a two-sided Student’s t-test (significant where $p < 0.05$) with the null hypothesis that the distributions of anomalies for the experiments forced with CMIP5 and CMIP6 SSTs (e.g. 4×CO₂-FULL_{CMIP5} − CTRL and 4×CO₂-FULL_{CMIP6} − CTRL) are statistically indistinguishable. An area weighted pattern correlation is used to quantify the similarity of the differences in the IGCM4 experiments with the MMM differences between CMIP5 and CMIP6 in different regions: 15°S–70°S in the South Pacific (150°E–290°E), South Atlantic (40°W–20°E) and Southern Indian Ocean (30°E–120°E) sectors.

3. Results

3.1. SH circulation response in CMIP5/6 models

Following Ceppi *et al* (2018), figure 1 shows the MMM annual mean $\Delta\phi_{EDJ}$ in the abrupt-4×CO₂ experiment as a function of GSAT change in CMIP5 and CMIP6 models. The CMIP6 models show



qualitatively similar behaviour to CMIP5, with the majority of the long-term poleward shift of ϕ_{EDJ} occurring in the first 10 years after the forcing is applied (93% and 78% of the TOTAL anomalies for CMIP5 and CMIP6, respectively). In the FAST period around 60% of the GSAT change takes place, after which relatively small changes in ϕ_{EDJ} occur, despite continued surface warming. Figure 1 also shows that, on average, the CMIP6 models warm by an additional 0.3 K ($\sim 10\%$) in the FAST period and by 0.8 K ($\sim 16\%$) for the TOTAL response, as compared to CMIP5. Interestingly, despite the larger surface warming on both FAST and SLOW timescales, the CMIP6 MMM annual mean $\Delta\phi_{EDJ}$ is smaller by 0.66° ($\sim 25\%$) in the FAST period ($p = 0.02$) and by 0.32° ($\sim 12\%$) for the TOTAL response, though the latter difference is nonsignificant ($p = 0.28$). A smaller FAST $\Delta\phi_{EDJ}$ in CMIP6 is found in all seasons, but is statistically significant in austral spring (September–November) and autumn (March–May) (see supplementary information figure S1). Interestingly, although there are statistically significant differences in the magnitude of the jet shift, the CMIP5 and CMIP6 models simulate, on average, equivalent increases in jet speed (see supplementary figure S2). We note that the significant correlation between the TOTAL annual mean $\Delta\phi_{EDJ}$ and GSAT response across CMIP5 models described by Grise and Polvani (2014) is nonsignificant in CMIP6 ($p = 0.12$) and does not hold for CMIP5 or CMIP6 models in the

FAST period (not shown). It therefore appears that the difference between the two generations of models cannot be explained by a response that is congruent with GSAT. We also note that the difference in jet shift between CMIP5 and CMIP6 models cannot be attributed to differences in the rapid adjustment to 4 \times CO₂ (i.e. the atmospheric response in the absence of SST changes). The MMM annual mean jet shift in the fixed-SST experiments performed in CMIP5 and CMIP6 is equivalent to 26% and 35% of the jet shift in the abrupt-4 \times CO₂ simulations, respectively, for the subset of models that provide fixed-SST simulations (see table S1). This is consistent with the rapid adjustment of the SH EDJ to CO₂-forcing found in previous studies (e.g. Wood *et al* 2020a). The difference between the MMM CMIP5 and CMIP6 rapid adjustment is nonsignificant in the annual mean and only shows a statistically significant smaller poleward jet shift in DJF and JJA (not shown), while the coupled experiments show statistically significant differences in MAM and SON (figure S1). This indicates that differences in the rapid adjustment to CO₂ in the absence of SST changes cannot account for the overall statistically significant differences in jet shift between the full CMIP5 and CMIP6 model ensembles. From hereon we focus on the differences in SH EDJ response between the CMIP5 and CMIP6 coupled models that emerge in the FAST period.

Figure 2 shows maps of the annual and seasonal mean MMM 850 hPa zonal wind anomalies in

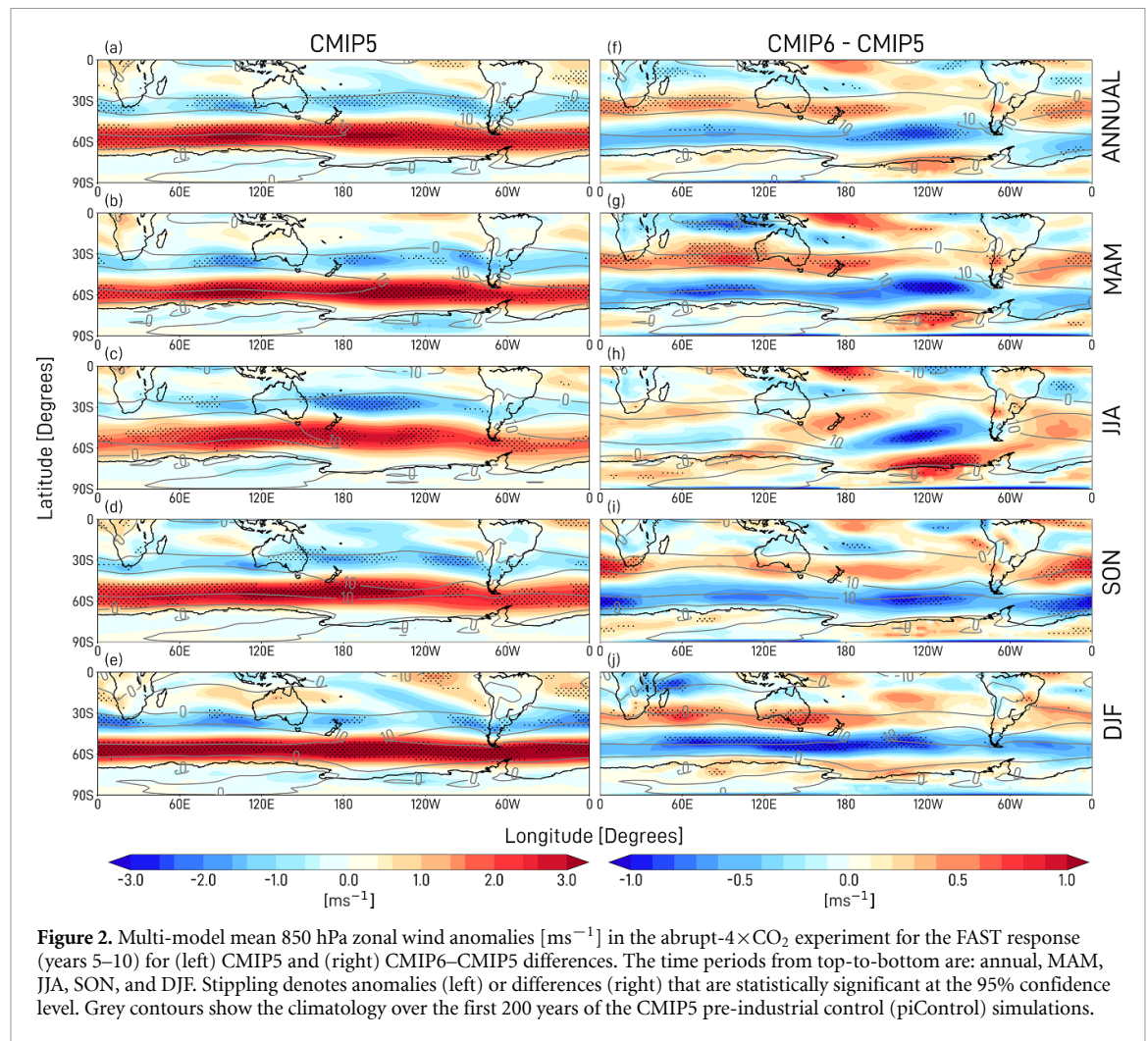


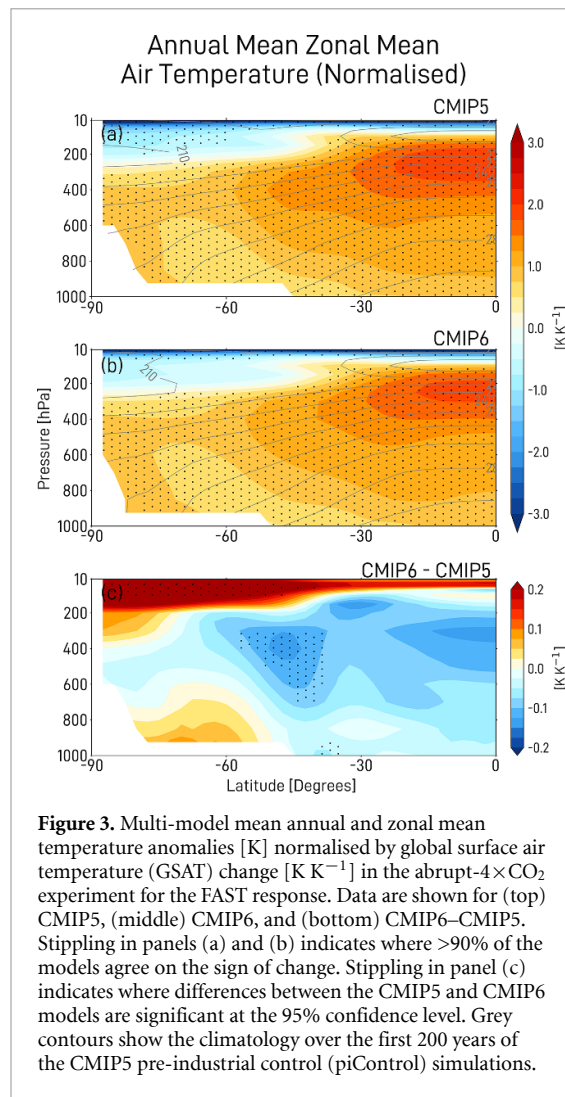
Figure 2. Multi-model mean 850 hPa zonal wind anomalies [ms^{-1}] in the abrupt- $4\times\text{CO}_2$ experiment for the FAST response (years 5–10) for (left) CMIP5 and (right) CMIP6–CMIP5 differences. The time periods from top-to-bottom are: annual, MAM, JJA, SON, and DJF. Stippling denotes anomalies (left) or differences (right) that are statistically significant at the 95% confidence level. Grey contours show the climatology over the first 200 years of the CMIP5 pre-industrial control (piControl) simulations.

the FAST period for (a)–(e) CMIP5 and (f)–(j) the difference between CMIP6 and CMIP5 models. In the annual mean, the CMIP5 wind anomalies show a dipole of strengthened and weakened westerlies on the poleward and equatorward side of the jet maximum, respectively, indicating a poleward shift of the jet at most longitudes. The differences between CMIP6 and CMIP5 show that the wind dipole is substantially reduced in CMIP6 at most longitudes and in all seasons other than JJA, where the greatest differences are found in the South Pacific sector with smaller differences elsewhere. The magnitude and significance of the differences varies by ocean basin and by season (see also supplementary information figures S1 and S3). This highlights the importance of evaluating the regional aspects of the SH EDJ response and not only the zonal mean which can mask locally significant differences. We return to this point later.

3.2. Temperature and SST responses in CMIP5/6 models

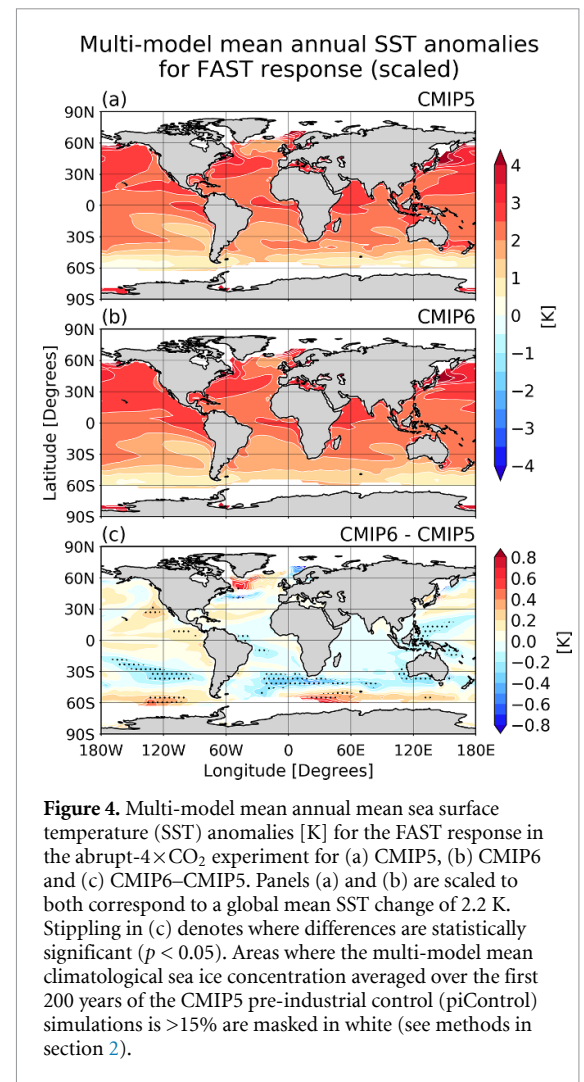
Figure 3 shows the MMM zonal and annual mean FAST air temperature changes in the SH for (a) CMIP5, (b) CMIP6 and (c) the CMIP6–CMIP5 differences. The values for each model are normalised by their respective GSAT change prior to averaging

to remove the effect of different ECS across models and therefore facilitate a comparison of the patterns of temperature response. The canonical pattern of temperature change to CO_2 forcing comprises stratospheric cooling that increases with height, amplified warming in the tropical upper troposphere and smaller amplification of tropospheric warming over Antarctica. The difference in the pattern of zonal mean temperature response per degree GSAT warming shows relatively weaker warming in the mid-troposphere between 30°S – 60°S and relatively weaker cooling in the midlatitude and polar lower stratosphere in CMIP6 as compared to CMIP5 models. This pattern is qualitatively similar throughout the year, though the weaker midlatitude warming is most pronounced in austral summer (DJF) and the weaker polar lower stratospheric cooling is most pronounced in austral winter and spring (JJA and SON) (see supplementary information figure S4). This pattern represents a smaller increase in equator-to-pole temperature gradient in the lower-to-mid troposphere in CMIP6 models compared to CMIP5, with the 850 hPa, 500 hPa and 250 hPa tropics-to-pole temperature gradient increases being 11%, 12% and 9% smaller per unit GSAT change respectively in CMIP6 compared to CMIP5. There is also a larger increase

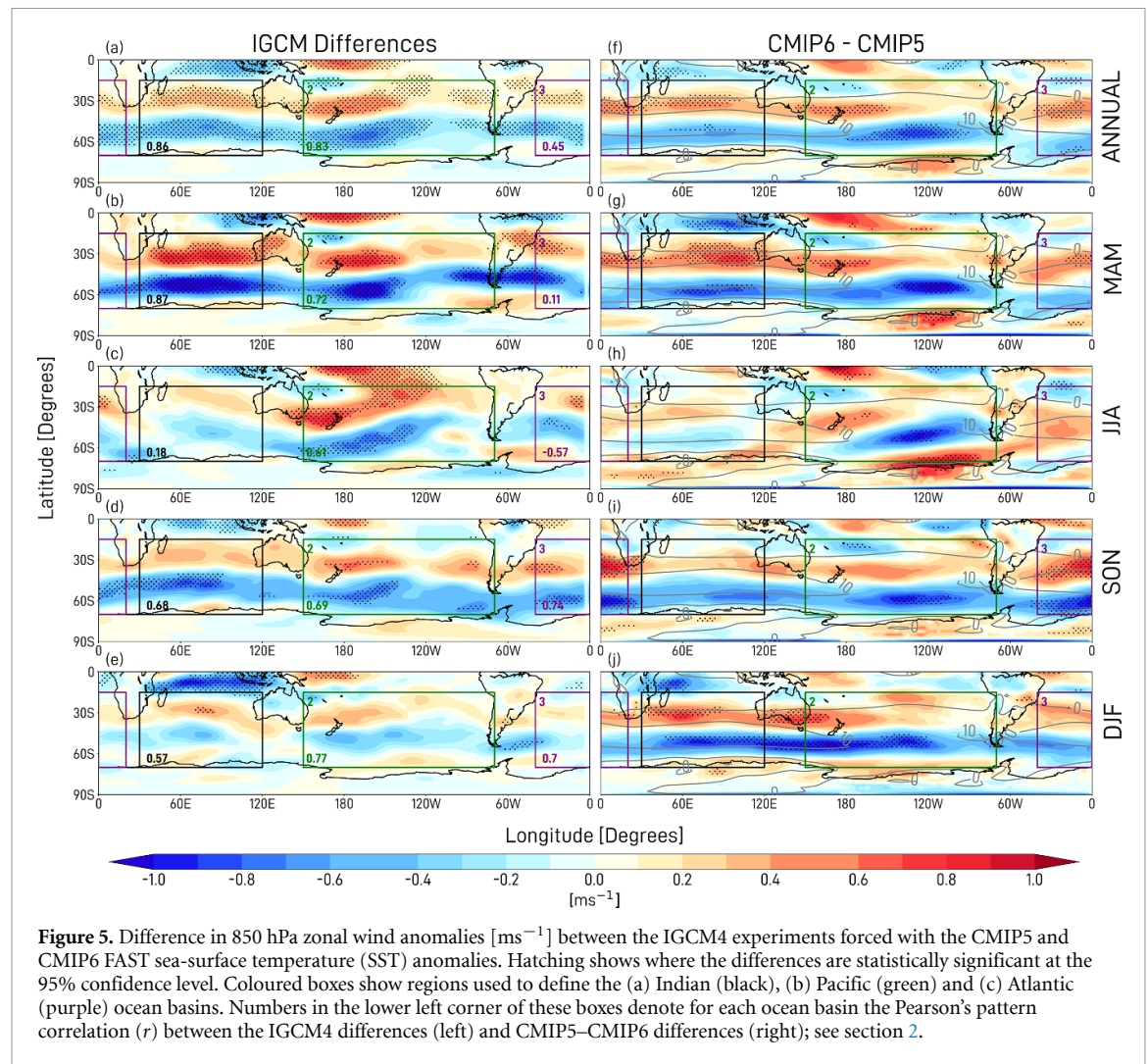


in equator-to-pole temperature gradient in the lower stratosphere above ~ 200 hPa in CMIP5 compared to CMIP6. Consistent with some previous studies (e.g. Harvey *et al* 2014, Grise and Polvani 2016; Wood *et al* 2020a), we find a statistically significant correlation ($p < 0.05$) between the intermodel spread of the absolute (non-GSAT-scaled) FAST lower tropospheric temperature gradient change and $\Delta\phi_{\text{EDJ}}$ in the CMIP5 and CMIP6 multi-model ensembles ($r = 0.45$ and 0.46 , respectively). A smaller increase in the tropospheric equator-to-pole temperature gradient in CMIP6 would therefore imply, on average, a weaker poleward jet shift as shown.

We next examine whether differences in simulated SST patterns between CMIP5 and CMIP6 models are consistent with the differences in tropospheric temperature gradient and jet shift. Figure 4 shows the MMM FAST SST response in (a) CMIP5, (b) CMIP6 and (c) the CMIP6–CMIP5 differences. Recall from section 2 that to facilitate a comparison of the patterns, the SST anomalies in each model are scaled to have the same global mean value. For reference the raw unscaled SSTs and their differences are shown in supplementary information figure S7. The canonical



pattern of FAST SST response, found in both CMIP5 and CMIP6 models, shows relatively larger warming in the tropics and weaker warming over the Southern Ocean; this pattern was highlighted by Ceppi *et al* (2018) as the cause of the proportionately large jet shift during the first decade after an abrupt CO_2 forcing is applied. Figure 4(c) shows that, on average, in the first decade there is weaker warming by up to 0.4 K locally between 30°S and 45°S and larger warming by up to 0.5 K locally between 45°S and 60°S in CMIP6 compared to CMIP5. This pattern reflects a more muted increase in the extratropical SST gradient, consistent with the more muted increase in lower-to-mid tropospheric temperature gradient. The CMIP6–CMIP5 difference in the peak-to-peak amplitude of the zonal mean FAST SST response between these latitude bands is 0.4 K, which is a substantial fraction ($\sim 30\%$) of the absolute MMM response in CMIP5 models (~ 1.4 K). In CMIP6 models, there is also a relatively larger decrease in the east-to-west SST gradient in the tropical Pacific by around 0.4 K and weaker warming by up to 0.2 K in the western tropical Atlantic, but both of these differences are only weakly significant. Investigation of the causes of the



differences in SST patterns is beyond the scope of the study; however, we note that the Southern Ocean meridional circulation helps shape the pattern of multi-decadal SST warming (e.g. Armour *et al* 2016) so it is possible this meridional circulation responds somewhat differently to CO_2 forcing in CMIP5 and CMIP6 models. Substantial differences in SH short-wave low cloud feedbacks have also been identified between CMIP5 and CMIP6 models (Zelinka *et al* 2020), and these are important for the surface energy budget over the Southern Ocean, which also influences SSTs.

3.3. IGCM4 simulations

We now use the IGCM4 model to isolate the impact of the differences in the abrupt- $4\times\text{CO}_2$ FAST SST patterns shown in figure 4 on the SH midlatitude circulation. Figures 5(a)–(e) show the differences in the 850 hPa zonal wind responses between the IGCM4 $4\times\text{CO}_2$ -FULL_{CMIP5} and $4\times\text{CO}_2$ -FULL_{CMIP6} experiments forced with the CMIP5 and CMIP6 SST anomalies from figures 4(a) and (b). For ease of comparison, the MMM FAST zonal wind differences between CMIP6 and CMIP5 models are also replotted

(figures 5(f)–(j)). The differences in low level zonal wind response due to the SST patterns imposed in IGCM4 bear a strong resemblance to the differences between CMIP6 and CMIP5 models. The pattern correlation between the IGCM4 and CMIP6/5 zonal wind differences in the region 15°S – 70°S are statistically significant throughout the year ($r = 0.76, 0.65, 0.64, 0.34, 0.67$ for the annual, DJF, MAM, JJA and SON means, respectively). The pattern correlations are particularly large ($r > 0.6$) in the South Pacific sector in all seasons, and in the southern Indian Ocean in the annual mean, MAM and SON. Conversely, the pattern correlations are relatively low in the Indian Ocean in JJA ($r = 0.18$), in the south Atlantic in MAM ($r = 0.11$) and is negative in south Atlantic JJA ($r = -0.57$).

The magnitude of the differences in zonal wind response in IGCM4 are also very similar to the CMIP6/5 differences in many regions and seasons, the main exception being in austral summer where the differences in SSTs induce substantially smaller zonal wind anomalies in IGCM4 than the CMIP6/5 differences (figures 5(e) vs. (j)). As described in the methods, SST field inputs to IGCM4 were rescaled to

a common global mean SST. This removes the influence of differences in SSTs owing to differences in climate sensitivity between CMIP5 and CMIP6 and thus isolates the role of the SST anomaly patterns alone. Further simulations (not shown) show the results from IGCM4 are largely insensitive to this choice of scaling, indicating that differences in global mean SST between CMIP5 and CMIP6 are of secondary importance for the SH circulation response. This finding is consistent with the fact that the CMIP6 models simulate, on average, a larger GSAT change, but a smaller jet shift than in CMIP5, so the reduction in circulation response is not congruent with GSAT.

When the southern extratropical (30°S – 90°S) SSTs are imposed in isolation (SHET-only_{CMIP5} and SHET-only_{CMIP6}), we find that IGCM4 simulates a poleward jet shift in both cases, but SHET-only_{CMIP6} induces a smaller poleward shift than SHET-only_{CMIP5}, with the magnitude of the difference being similar to that shown in the $4\times\text{CO}_2$ -FULL simulations (see blue markers in supplementary figures S1 and S3). Note that the absolute magnitude of poleward jet shift in SHET-only is somewhat different to $4\times\text{CO}_2$ -FULL owing to the nature of the experiment which fixes SSTs outside the SH extratropics thus altering the temperature flux between ocean and atmosphere. Furthermore, both the $4\times\text{CO}_2$ -FULL and SHET-only experiments simulate similar patterns of differences in zonal mean air temperature to the CMIP results, with a relatively weaker warming in the southern midlatitude troposphere using CMIP6 SSTs as compared to CMIP5 SSTs (compare supplementary figures S5(c) and S6(c) to figure 3(c)). This further suggests an important role for the pattern of zonal mean temperature changes induced by the different SST anomaly patterns.

4. Discussion and conclusions

An intermediate complexity general circulation model (IGCM4) forced with multi-model mean SST patterns and a quadrupling in CO_2 is able to quantitatively reproduce many of the differences in lower tropospheric zonal wind responses between CMIP5 and CMIP6 models. The main exception is in austral summer when the SSTs induce relatively weak zonal wind anomalies compared to the CMIP6/5 differences. The differences are similarly reproduced by IGCM4 when only the SH extratropical SSTs from CMIP5 and CMIP6 models are imposed alone. These results support the hypothesis that differences in SST patterns can explain a substantial fraction of the regional differences in the response of SH extratropical circulation to CO_2 forcing between CMIP5 and CMIP6 models. This is an alternative hypothesis to Curtis *et al* (2020) who attributed the smaller SH jet shift in response to $4\times\text{CO}_2$ during the extended austral winter (May–October) to improvements in model

climatologies in CMIP6, and specifically a reduced equatorward bias in the location of the SH jet.

The approach used to isolate the impacts of SSTs on the SH EDJ assumes that the differences in SST patterns between CMIP5/6 are independent of the differences in the SH circulation itself. Ferreira *et al* (2015) showed in a model that the short-term (years 1–5) SH extratropical SST response to a positive SAM anomaly (i.e. a poleward shift in midlatitude westerlies)—forced by an imposed ozone hole—comprises a cooling at high latitudes and warming in midlatitudes during the first decade. It is therefore possible that part of the extratropical dipole pattern of SST difference between CMIP6 and CMIP5 models is a consequence of the poleward jet shift being more muted in CMIP6. However, we estimate that the magnitude of the differences in SST patterns is larger than can be explained by the differences in surface wind anomalies alone (compare figure S8(a) which generally shows maximum SST anomalies of $\sim 0.3\text{ K}$ and wind anomalies of $\sim 0.4\text{ ms}^{-1}$ with the top left panel of figure 4 in Ferreira *et al* (2015) which generally shows maximum SST anomalies of $\sim 0.5\text{ K}$ and wind anomalies of $\sim 2\text{ ms}^{-1}$). Furthermore, it would be extremely surprising if a pattern of SST anomalies forced by atmospheric circulation happened to produce a very similar atmospheric response when imposed separately. We therefore speculate that the differences in SST warming patterns between CMIP5/6 models are related to other processes that could include ocean circulation response to warming and/or Southern Ocean cloud feedbacks. An investigation of the ocean response is beyond the scope of this study, but would be an interesting topic for future work.

Data Availability Statement

The data that support the findings of this study are openly available at the following URL/DOI: <http://doi.org/10.5281/zenodo.4250119> (Wood *et al* 2020b).

Acknowledgments


TW was funded by a PhD studentship from the NERC SPHERES Doctoral Training Partnership (NE/L002574/1). CMM and ACM were funded by the European Union's Horizon 2020 Research and Innovation Programme under grant agreement 820829 (CONSTRAIN). ACM was funded by a NERC Independent Research Fellowship (NE/M018199/1). AC and ACM were supported by the Leverhulme Trust. The IGCM4 experiments were conducted on ARC4, part of the High Performance Computing facilities at the University of Leeds, UK. We are grateful to Michelle McCrystall for providing a Python code used for the cosine smoothing of SST anomalies in some

experiments. We acknowledge the World Climate Research Programme, which, through its Working Group on Coupled Modelling, coordinated and promoted CMIP. We thank the climate modelling groups for producing and making available their model output; the Earth System Grid Federation (ESGF) and UK Centre for Environmental Data Analytics (CEDA) JASMIN cluster for archiving the data and providing access; and the multiple funding agencies who support CMIP, ESGF, and CEDA/JASMIN. The authors thank Alex Sen Gupta and one anonymous reviewer for their constructive comments which improved the manuscript.

ORCID iDs

Tom Wood  <https://orcid.org/0000-0002-6049-5805>

Christine M McKenna  <https://orcid.org/0000-0002-9677-4582>

Andreas Chrysanthou  <https://orcid.org/0000-0002-8670-5436>

Amanda C Maycock  <https://orcid.org/0000-0002-6614-1127>

References

- Andrews T, Gregory J M, Webb M J and Taylor K E 2012 Forcing, feedbacks and climate sensitivity in CMIP5 coupled atmosphere-ocean climate models *Geophys. Res. Lett.* **39** L09712
- Armour K, Marshall J, Scott J, Donohoe A and Newsom E R 2016 Southern Ocean warming delayed by circumpolar upwelling and equatorward transport *Nat. Geosci.* **9** 549–54
- Barnes E A and Polvani L 2013 Response of the midlatitude jets, and of their variability, to increased greenhouse gases in the CMIP5 models *J. Clim.* **26** 7117–35
- Bracegirdle T J, Hyder P and Holmes C R 2018 CMIP5 diversity in southern westerly jet projections related to historical sea ice area: strong link to strengthening and weak link to shift *J. Clim.* **31** 195–211
- Bracegirdle T J, Shuckburgh E, Saltee J - B, Wang Z, Meijers A J S, Bruneau N, Phillips T and Wilcox L J 2013 Assessment of surface winds over the Atlantic, Indian, and Pacific Ocean sectors of the Southern Ocean in CMIP5 models: historical bias, forcing response, and state dependence *J. Geophys. Res. Atmos.* **118** 547–62
- Ceppi P, Zappa G, Shepherd T G and Gregory J M 2018 Fast and slow components of the extratropical atmospheric circulation response to CO₂ forcing *J. Clim.* **31** 1091–105
- Curtis P E, Ceppi P and Zappa G 2020 Role of the mean state for the Southern Hemispheric jet stream response to CO₂ forcing in CMIP6 models *Environ. Res. Lett.* **15** 64011
- Eyring V, Bony S, Meehl G A, Senior C A, Stevens B, Stouffer R J and Taylor K E 2016 Overview of the Coupled Model Intercomparison Project Phase 6 (CMIP6) experimental design and organization *Geosci. Model Dev.* **9** 1937–58
- Ferreira D, Marshall J, Bitz C M, Solomon S and Plumb A 2015 Antarctic Ocean and sea ice response to ozone depletion: a two-time-scale problem *J. Clim.* **28** 1206–26
- Forster P M, Maycock A C, McKenna C M and Smith C J 2020 Latest climate models confirm need for urgent mitigation *Nat. Clim. Change* **10** 7–10
- Gillett N P, Kell T D and Jones P D 2006 Regional climate impacts of the Southern Annular Mode *Geophys. Res. Lett.* **33** L23704
- Grise K M and Polvani L M 2014 Is climate sensitivity related to dynamical sensitivity? A Southern Hemisphere perspective *Geophys. Res. Lett.* **41** 534–40
- Grise K M and Polvani L M 2016 Is climate sensitivity related to dynamical sensitivity? *J. Geophys. Res. Atmos.* **121** 5159–76
- Grise K M and Polvani L M 2017 Understanding the time scales of the tropospheric circulation response to abrupt CO₂ forcing in the Southern Hemisphere: seasonality and the role of the Stratosphere *J. Clim.* **30** 8497–515
- Harvey B J, Shaffrey L C and Woollings T J 2014 Equator-to-pole temperature differences and the extra-tropical storm track responses of the CMIP5 climate models *Clim. Dyn.* **43** 1171–82
- Holland M M, Landrum L, Kostov Y and Marshall J 2017 Sensitivity of Antarctic sea ice to the Southern Annular Mode in coupled climate models *Clim. Dyn.* **49** 1813–31
- Hoskins B J and Simmons A J 1975 A multilayer spectral model and the semi-implicit method *Q. J. R. Meteorol. Soc.* **101** 637–55
- Joshi M, Stringer M, van der Wiel K, O'Callaghan A and Fueglistaler S 2015 IGCM4: a fast, parallel and flexible intermediate climate model *Geosci. Model Dev.* **8** 1157–67
- Kang S M, Polvani L M, Fyfe J C and Sigmond M 2011 Impact of polar ozone depletion on subtropical precipitation *Science* **332** 951–4
- Karpechko A Y, Gillett N P, Marshall G J and Screen J A 2009 Climate impacts of the Southern Annular Mode simulated by the CMIP3 models *J. Clim.* **22** 3751–68
- Lim E - P, Hendon H H, Arblaster J M, Delage F, Nguyen H, Min S - K and Wheeler M C 2016 The impact of the Southern Annular Mode on future changes in Southern Hemisphere rainfall *Geophys. Res. Lett.* **43** 7160–7
- Lu J, Vecchi G A and Reichler T 2007 Expansion of the Hadley cell under global warming *Geophys. Res. Lett.* **34** L06805
- Mccrystal M R, Hosking J S, White I P and Maycock A C 2020 The impact of changes in tropical sea surface temperatures over 1979–2012 on Northern Hemisphere high-latitude climate *J. Clim.* **33** 5103–21
- O'Callaghan A, Joshi M, Stevens D and Mitchell D 2014 The effects of different sudden stratospheric warming type on the ocean *Geophys. Res. Lett.* **41** 7739–45
- Simpson I R and Polvani L M 2016 Revisiting the relationship between jet position, forced response, and annular mode variability in the southern midlatitudes *Geophys. Res. Lett.* **43** 2896–903
- Taylor K E, Stouffer R J and Meehl G A 2012 An overview of CMIP5 and the experiment design *Bull. Am. Meteorol. Soc.* **93** 485–98
- Thorncroft C D, Hoskins B J and McIntyre M E 1993 Two paradigms of baroclinic-wave life-cycle behaviour *Q. J. R. Meteorol. Soc.* **119** 17–55
- Waugh D W, Banerjee A, Fyfe J C and Polvani L M 2020 Contrasting recent trends in Southern Hemisphere Westerlies across different ocean basins *Geophys. Res. Lett.* **47**
- Winter B and Bourqui M S 2011 Sensitivity of the stratospheric circulation to the latitude of thermal surface forcing *J. Clim.* **24** 5397–415
- Wood T et al 2020a The Southern Hemisphere midlatitude circulation response to rapid adjustments and sea surface temperature driven feedbacks *J. Clim.* **33** 9673–90
- Wood T, McKenna C M, Chrysanthou A and Maycock A C 2020b Role of sea surface temperature patterns for the Southern Hemisphere jet stream response to CO₂ forcing *Zenodo* (<https://doi.org/10.5281/zenodo.4250119>)
- Zelinka M D, Myers T A, McCoy D T, Po-Chedley S, Caldwell P M, Ceppi P, Klein S A and Taylor K E 2020 Causes of higher climate sensitivity in CMIP6 models *Geophys. Res. Lett.* **47** e2019GL085782